AD_____

Award Number: DAMD17-02-1-0018

TITLE: Molecular Study of BAG Domains: A New Motif in Prostate Cancer

PRINCIPAL INVESTIGATOR: Klara Briknarova, Ph.D.

CONTRACTING ORGANIZATION: The Burham Institute
La Jolla, CA 92037

REPORT DATE: September 2003

TYPE OF REPORT: Annual Summary

PREPARED FOR: U.S. Army Medical Research and Materiel Command
Fort Detrick, Maryland 21702-5012

REPORT DOCUMENTATION PAGE

Form Approved
OMB No. 074-0188

1. AGENCY USE ONLY (Leave blank)	2. REPORT DATE	3. REPORT TYPE AND DATES COVERED
	September 2003	Annual Summary (1 Sep 02 - 31 Aug 03)

4. TITLE AND SUBTITLE
Molecular Study of BAG Domains: A New Motif in Prostate Cancer

5. FUNDING NUMBERS
DAMD17-02-1-0018

6. AUTHOR(S)
Klara Briknarova, Ph.D.

7. PERFORMING ORGANIZATION NAME(S) AND ADDRESS(ES)
The Burnham Institute
La Jolla, CA 92037

E-Mail: klara@burnham.org

8. PERFORMING ORGANIZATION REPORT NUMBER

9. SPONSORING / MONITORING AGENCY NAME(S) AND ADDRESS(ES)
U.S. Army Medical Research and Materiel Command
Fort Detrick, Maryland 21702-5012

10. SPONSORING / MONITORING AGENCY REPORT NUMBER

11. SUPPLEMENTARY NOTES
Original contains color plates: ALL DTIC reproductions will be in black and white

12a. DISTRIBUTION / AVAILABILITY STATEMENT
Approved for Public Release; Distribution Unlimited

12b. DISTRIBUTION CODE

13. ABSTRACT (Maximum 200 Words)

The "BAG" domain is found in BAG family proteins and may have relevance to prostate cancer resistance to hormone-ablative and anti-androgen therapy. It promotes tumor survival and aggressiveness through a variety of mechanisms, including interactions with the anti-apoptotic protein Bcl-2 and Hsp70/Hsc70 molecular chaperones. Using NMR spectroscopy and computational methods, we have determined the structure of the BAG domain from BAG4 and compared it with its counterpart in BAG1. The difference is striking, and the structural comparison defines two subfamilies of human BAG proteins. One subfamily includes BAG1, and the other is represented by BAG3, BAG4 and BAG5 proteins. BAG domains from both BAG1 and BAG4 are three-helix bundles; however, in BAG1, each helix in this bundle is three to four turns longer than its counterpart in BAG4, which increases the length of the domain by one-half. We have also investigated the interactions of BAG domains with Hsp70/Hsc70 proteins, using NMR and site-directed mutagenesis. Despite their distinct sizes, BAG domains from BAG1 and BAG4 interact with Hsc70 in an analogous manner. Our structural studies provide context for functional investigations and enable us to better understand the role of BAG proteins at the molecular level.

14. SUBJECT TERMS
BAG1, BAG domain, BAG4, SODD, Bcl-2, NMR, structural biology

15. NUMBER OF PAGES
14

16. PRICE CODE

17. SECURITY CLASSIFICATION OF REPORT	18. SECURITY CLASSIFICATION OF THIS PAGE	19. SECURITY CLASSIFICATION OF ABSTRACT	20. LIMITATION OF ABSTRACT
Unclassified	Unclassified	Unclassified	Unlimited

Table of Contents

Introduction

BAG proteins share a conserved protein interaction motif, called the "BAG" domain, which binds to Hsp70/Hsc70 molecular chaperones and modulates their activity. Members of the BAG family also interact with and regulate the function of the anti-apoptotic proteins Bcl-2 and Bcl-X_L, and several signal transducing proteins and transcription factors, including the androgen receptor. BAG proteins suppress cell death, play an important role in cell signaling pathways, and may promote tumor growth and aggressiveness by a variety of mechanisms. The long isoform of BAG1, BAG1L, allows androgen receptor activation with lower levels of 5α-dihydrotestosterone and in the presence of the anti-androgen cyproterone acetate. This indicates that BAG proteins may have relevance to mechanisms of prostate cancer resistance to hormone-ablative and anti-androgen therapy. In order to understand the role that the BAG domains play in interactions with other proteins, it is necessary to elucidate the molecular mechanism of their actions. In our research, we use nuclear magnetic resonance (NMR) spectroscopy to address two different functional aspects of BAG domain structure. We have determined structures of BAG domains from different members of the BAG family and compared their structural and functional features. We will also define molecular contacts of the BAG domain of BAG1 with Bcl-X_L and compare and contrast the interactions with those between BAG1 and Hsc70.

Body

Task1: Interaction of BAG domain from BAG1 with Bcl-X_L and other proteins

Bcl-family members heterodimerize with Bcl-X_L via their conserved sequence, termed BH3 [1;2]. BH3-like sequences have also been identified in the BAG domains of several BAG-family proteins [3]. However, most BAG residues in this motif that would be expected to interact with Bcl-X_L, based on comparison with the Bcl-X_L/Bak or Bad peptide complexes [1;2], are buried in the core of the three-helix bundle, as revealed by our structural studies described below [4;5]. Consistent with that, we were unable to detect any binding of Bcl-X_L to the BAG domain of BAG1 using purified proteins expressed in *E. coli*. Interestingly, BH3-like residues involved in interaction with Bcl-X_L are also buried in most unbound Bcl-family proteins [6;7;8] and only partially exposed in others [9;10]. Hence, heterodimerization of Bcl proteins seems to require structural rearrangement.

To test whether the BH3-like region from BAG-family proteins can bind to Bcl-2 and Bcl-X_L, we obtained synthetic peptides corresponding to this region of BAG1 and BAG4. However, ELISA and fluorescence anisotropy competition assays using these peptides, Bcl-2 or Bcl-X_L proteins and labeled Bad peptide are so far not definitive. Now, with the peptides in hand, we are in the process of acquiring ^{15}N-labeled Bcl-X_L to assess the binding using NMR.

Task2: Structure of the BAG domain from BAG4 and comparison with BAG1

Task 2 has been completed (see Briknarová et al., 2002 in Appendix for details). Using NMR spectroscopy and computational methods, we have determined the structure of the

BAG domain from BAG4 and compared it to its counterpart in BAG1 [4]. The difference between BAG domains from BAG1 and BAG4 is striking, and the structural comparison defines two subfamilies of human BAG proteins. One subfamily includes BAG1, and the other is represented by the closely related BAG3, BAG4 and BAG5 proteins, which contain a structurally and evolutionarily distinct BAG domain. BAG domains from both BAG1 and BAG4 are three-helix bundles; however, in BAG1, each helix in this bundle is three to four turns longer than its counterpart in BAG4, which increases the length of the domain by one-half. We have also investigated the interactions of BAG domains with Hsp70/Hsc70 proteins, using NMR and site-directed mutagenesis. Despite their distinct sizes, BAG domains from BAG1 and BAG4 interact with Hsc70 in an analogous manner.

Key Research Accomplishments

- Assignment of ^{1}H, ^{13}C and ^{15}N chemical shifts of the BAG domain from human BAG4
- Determination of the solution structure of the BAG domain from human BAG4
- Characterization of Hsc70 binding interface on BAG4 using NMR-monitored titrations and site-directed mutagenesis
- Comprehensive comparison of BAG domains from human BAG-family proteins

Reportable Outcomes

- Briknarová, K., Takayama, S., Homma, S., Baker, K., Cabezas, E., Hoyt, D. W., Li, Z., Satterthwait, A. C. & Ely, K. R. (2002). BAG4/SODD protein contains a short BAG domain. *J. Biol. Chem.* **277**, 31172-31178.
- The atomic coordinates (code 1M62) have been deposited in the Protein Data Bank, Research Collaboratory for Structural Bioinformatics, Rutgers University, New Brunswick, NJ (http://www.rcsb.org).

Conclusions

BAG proteins represent a new regulatory pathway in prostate cancer. Our structural studies provide context for functional investigations and enable us to understand the role of BAG proteins in prostate cancer at the molecular level. BAG proteins may become a target for novel therapeutic strategies, and the availability of molecular models that reveal both similarities and differences among the BAG domains will streamline the drug development process.

References

1. Sattler, M., Liang, H., Nettesheim, D., Meadows, R. P., Harlan, J. E., Eberstadt, M., Yoon, H. S., Shuker, S. B., Chang, B. S., Minn, A. J., Thompson, C. B. & Fesik, S. W. (1997). Structure of Bcl-x_L-Bak peptide complex: Recognition between regulators of apoptosis. *Science* 275, 983-986.
2. Petros, A. M., Nettesheim, D. G., Wang, Y., Olejniczak, E. T., Meadows, R. P., Mack, J., Swift, K., Matayoshi, E. D., Zhang, H., Thompson, C. B. & Fesik, S. W. (2000). Rationale for Bcl-x_L/Bad peptide complex formation from structure, mutagenesis, and biophysical studies. *Protein Sci.* 9, 2528-2534.

3. Antoku, K., Maser, R. S., Scully, W. J. J., Delach, S. M. & Johnson, D. E. (2001). Isolation of Bcl-2 binding proteins that exhibit homology with BAG-1 and suppressor of death domains protein. *Biochem. Biophys. Res. Commun.* 286, 1003-1010.
4. Briknarová, K., Takayama, S., Brive, L., Havert, M. L., Knee, D. A., Velasco, J., Homma, S., Cabezas, E., Stuart, J., Hoyt, D. W., Satterthwait, A. C., Llinás, M., Reed, J. C. & Ely, K. R. (2001). Structural analysis of BAG1 cochaperone and its interactions with Hsc70 heat shock protein. *Nat. Struct. Biol.* 8, 349-352.
5. Briknarová, K., Takayama, S., Homma, S., Baker, K., Cabezas, E., Hoyt, D. W., Li, Z., Satterthwait, A. C. & Ely, K. R. (2002). BAG4/SODD protein contains a short BAG domain. *J. Biol. Chem.* 277, 31172-31178.
6. Suzuki, M., Youle, R. J. & Tjandra, N. (2000). Structure of Bax: Coregulation of dimer formation and intracellular localization. *Cell* 103, 645-654.
7. Muchmore, S. W., Sattler, M., Liang, H., Meadows, R. P., Harlan, J. E., Yoon, H. S., Nettesheim, D., Chang, B. S., Thompson, C. B., Wong, S. L., Ng, S. C. & Fesik, S. W. (1996). X-ray and NMR structure of human Bcl-x_L, an inhibitor of programmed cell death. *Nature* 381, 335-341.
8. Petros, A. M., Medek, A., Nettesheim, D., Kim, D. H., Yoon, H. S., Swift, K., Matayoshi, E. D., Oltersdorf, T. & Fesik, S. W. (2001). Solution structure of the antiapoptotic protein bcl-2. *Proc. Natl. Acad. Sci. USA* 98, 3012-3017.
9. Chou, J. J., Li, H., Salvesen, G. S., Yuan, J. & Wagner, G. (1999). Solution structure of BID, an intracellular amplifier of apoptotic signaling. *Cell* 96, 615-624.
10. McDonnell, J. M., Fushman, D., Milliman, C. L., Korsmeyer, S. J. & Cowburn, D. (1999). Solution structure of the proapoptotic molecule BID: A structural basis for apoptotic agonists and antagonists. *Cell* 96, 625-634.

APPENDIX COVER SHEET

THE JOURNAL OF BIOLOGICAL CHEMISTRY

Vol. 277, No. 34, Issue of August 23, pp. 31172–31178, 2002
Printed in U.S.A.

BAG4/SODD Protein Contains a Short BAG Domain*

Received for publication, March 22, 2002, and in revised form, May 8, 2002
Published, JBC Papers in Press, June 10, 2002, DOI 10.1074/jbc.M202792200

Klára Briknarová‡, Shinichi Takayama‡, Sachiko Homma‡, Kelly Baker‡, Edelmira Cabezas‡, David W. Hoyt§, Zhen Li‡, Arnold C. Satterthwait‡, and Kathryn R. Ely‡¶

From ‡The Burnham Institute, La Jolla, California 92037 and §Environmental Molecular Sciences Laboratory, Pacific Northwest National Laboratory, Richland, Washington 99352

BAG (Bcl-2-associated athanogene) proteins are molecular chaperone regulators that affect diverse cellular pathways. All members share a conserved motif, called the BAG domain (BD), which binds to Hsp70/Hsc70 family proteins and modulates their activity. We have determined the solution structure of BD from BAG4/SODD (silencer of death domains) by multidimensional nuclear magnetic resonance methods and compared it to the corresponding domain in BAG1 (Briknarová, K., Takayama, S., Brive, L., Havert, M. L., Knee, D. A., Velasco, J., Homma, S., Cabezas, E., Stuart, J., Hoyt, D. W., Satterthwait, A. C., Llinás, M., Reed, J. C., and Ely, K. R. (2001) *Nat. Struct. Biol.* 8, 349–352). The difference between BDs from these two BAG proteins is striking, and the structural comparison defines two subfamilies of mammalian BD-containing proteins. One subfamily includes the closely related BAG3, BAG4, and BAG5 proteins, and the other is represented by BAG1, which contains a structurally and evolutionarily distinct BD. BDs from both BAG1 and BAG4 are three-helix bundles; however, in BAG4, each helix in this bundle is three to four turns shorter than its counterpart in BAG1, which reduces the length of the domain by one-third. BAG4 BD thus represents a prototype of the minimal functional fragment that is capable of binding to Hsc70 and modulating its chaperone activity.

BAG[1] proteins are conserved throughout eukaryotes, with homologues found in vertebrates, insects, nematodes, yeast, and plants (1–3). The human members of this family include BAG1 (4), BAG2 (1), BAG3 (CAIR-1/Bis) (1, 5, 6), BAG4 (SODD) (1, 7), BAG5 (1), and BAG6 (BAT3/Scythe) (8–10) (Fig. 1). BAG proteins contain diverse N-terminal sequences but share a conserved protein interaction module near the C-terminal end called the BAG domain (BD). The BD binds to the ATPase domain of Hsp70/Hsc70 and modulates activity of these molecular chaperones (11, 12). The BD of BAG1 also interacts with the C-terminal catalytic domain of Raf-1 and activates the kinase (13). It has been proposed that BAG family members serve as "toggles" in cell signaling pathways (10). For example, Raf-1 and Hsp70 may compete for binding to BAG1 (14). When levels of Hsp70 are elevated after cell stress, the BAG1·Raf-1 complex is replaced by BAG1·Hsp70, and DNA synthesis is inhibited (14). Thus, BAG1 serves as a molecular switch between cell proliferation and growth arrest. BAG4 (SODD), on the other hand, may play a role as a cellular "adaptor." It has been speculated that BAG4 recruits Hsc70 to tumor necrosis factor receptor 1 (TNFR1) and death receptor 3 (DR3) (2, 7), inducing conformational changes that prevent receptor signaling in the absence of ligand.

Each of the human BAG proteins binds to Hsp70/Hsc70 and modulates their chaperone activity. The conserved BD is necessary and sufficient for this interaction (1, 11).[2] Here we report the solution structure of the BD of BAG4 and its comparison with the BD of BAG1 (3, 15). The BD in BAG4 is significantly shorter than its counterpart in BAG1 and may define a minimal structural unit that binds Hsp70/Hsc70. Our comparison reveals two subfamilies of BAG proteins that are structurally and evolutionarily distinct.

EXPERIMENTAL PROCEDURES

NMR Spectroscopy and Structure Calculation—BAG4 BD (residues 376–457) was expressed in *Escherichia coli* as a glutathione transferase (GST) fusion construct. After initial purification of the recombinant protein by affinity chromatography on glutathione-agarose resin, the GST moiety was removed by thrombin cleavage, and the digest was separated using glutathione-agarose. Remaining impurities were eliminated by affinity chromatography on a benzamidine-agarose column and by ion-exchange chromatography on a Q-Sepharose column. NMR samples contained 1–2 mM ^{15}N- or $^{13}C/^{15}N$-labeled protein, 10 mM potassium phosphate buffer, pH 7.2, 100 mM KCl, 1 mM DTT, and 1 mM EDTA in 90% H_2O/10% D_2O. Spectra were acquired at 30 °C on Varian 500, 600, and 750 MHz spectrometers. The data were processed and analyzed with Felix 2000 (Molecular Simulations, Inc., San Diego). ^{1}H, ^{15}N, and ^{13}C assignments were established based on CBCA(CO)NH, HNCACB, HNCO, C(CO)NH, H(CCO)NH, HCCH-TOCSY, and three-dimensional ^{15}N-edited NOESY. Distance restraints were obtained from three-dimensional ^{15}N-edited NOESY and three-dimensional $^{13}C/^{15}N$-edited NOESY. φ and ψ dihedral angle restraints were generated with TALOS (16). Structures were calculated with standard torsion angle dynamics (TAD) simulated annealing protocol implemented in CNS 1.0 (17) using restraints for 1153 interproton distances (120 long range, $5 \leq$ i-j, 199 medium-range, $2 \leq$ i-j ≤ 4, 195 sequential and 639 intraresidual), 92 hydrogen bond distances, and 61 φ and 61 ψ dihedral angles. The protocol consisted of high temperature TAD, followed by TAD and cartesian slow cooling stages and final minimization. The scale factor for the dihedral angle energy term was doubled throughout the calculation; otherwise, default parameters were employed. Of 28 structures, 25 structures were selected that had no distance and dihedral angle restraint violated by more than 0.5 Å or 5°, respectively. The statistics are summarized in Table I. The structure with the lowest energy was used for illustrations and discussion. All figures were generated with MOLMOL 2K.1 (18).

* This work was supported by NCI, National Institutes of Health Grant CA 67329, the USAMRMC Prostate Cancer Program (DAMD 17-99-1-9094 and PC010678), and the University of California Breast Cancer Research Program (7FB-0084). The costs of publication of this article were defrayed in part by the payment of page charges. This article must therefore be hereby marked "*advertisement*" in accordance with 18 U.S.C. Section 1734 solely to indicate this fact.

The atomic coordinates and structure factors (code 1M62) have been deposited in the Protein Data Bank, Research Collaboratory for Structural Bioinformatics, Rutgers University, New Brunswick, NJ (http://www.rcsb.org/).

¶ To whom correspondence should be addressed. Tel.: 858-646-3135; Fax: 858-646-3191; E-mail: ely@burnham.org.

[1] The abbreviations used are: BAG, Bcl-2-associated athanogene; SODD, silencer of death domains; BD, Bag domain; GST, glutathione *S*-transferase; TAD, torsion angle dynamics; PDB, protein data bank.

[2] S. Takayama, unpublished results.

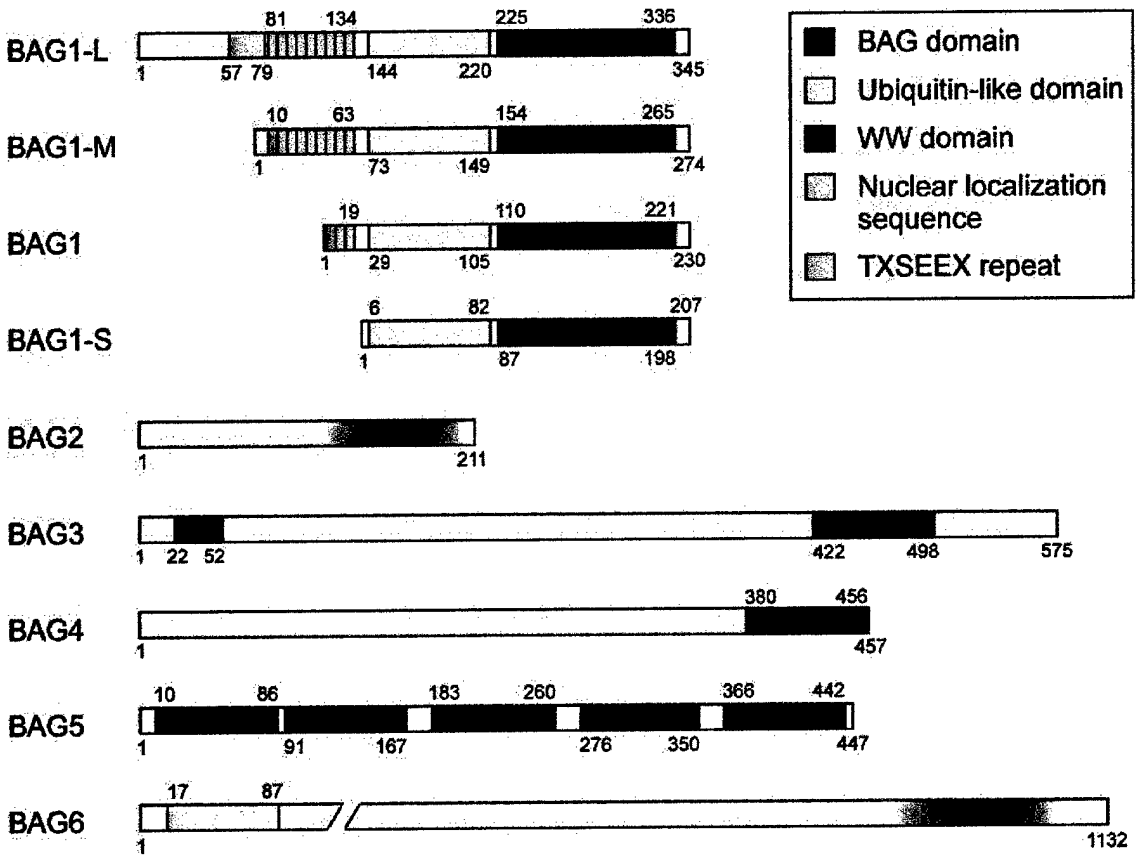

FIG. 1. **Domain structure of human BAG family proteins.** The positions of the BAG domain (*red*), ubiquitin-like domain (*yellow*), WW domain (*blue*), nuclear localization sequence (*cyan*), and TXSEEX repeats (*green*) in human BAG family members are indicated. Boundaries of the putative BAG domains in BAG2 and BAG6 are not known. Four isoforms of the BAG1 protein have been identified (25, 26) and are denoted BAG1-L, BAG1-M, BAG1, and BAG1-S.

TABLE I
Structural statistics for BAG4

Structural statistics for BAG4	
Root mean square deviation (RMSD) from experimental restraints	
NOE distance restraints (Å)	0.016 ± 0.001
dihedral angle restraints (°)	0.26 ± 0.02
RMSD from idealized geometry (17)	
bonds (Å)	0.0018 ± 0.0001
angles (°)	0.38 ± 0.02
impropers (°)	0.28 ± 0.02
RMSD of residues 380–399, 407–423, 432–456 (helical regions) from mean coordinates[a]	
backbone atoms (N, C^α, C) (Å)	0.58 ± 0.14
heavy atoms (Å)	1.21 ± 0.10
RMSD of residues 376–457 from mean coordinates[a]	
backbone atoms (N, C^α, C) (Å)	0.82 ± 0.18
heavy atoms (Å)	1.32 ± 0.11
Distribution of φ, ψ dihedral angles of residues 376–457 in Ramachandran plot (28)	
the most favored regions (%)	94.3
additional allowed regions (%)	4.3
generously allowed regions (%)	0.6
disallowed regions (%)	0.7

[a] Mean coordinates were obtained by averaging coordinates of 25 calculated structures, which were first superposed using backbone atoms (N, C^α, C) of the helical regions (residues 380–399, 407–423, and 432–456).

Peptide Synthesis and Binding Study—The peptide corresponding to helical region Asn-256–Cys-267 of the ATPase domain of human Hsc70, which was predicted to bind to BAG4, was synthesized in a helix-nucleated form to stabilize helicity (19) and characterized as described previously (15). ^1H-^{15}N HSQC spectra were recorded for ^{15}N-labeled BAG4 solutions containing varying concentrations of peptide, and most pronounced resonance shifts of BAG4 amides were noted and mapped onto the structure.

Mutational Analysis of BAG4 Binding to Hsc70—Mutations in BAG4 were generated by two-step PCR-based mutagenesis using a full-length human BAG4 cDNA (1) as a template (15). The following forward (f) and reverse (r) primers were used: GGGAATTCACTCCTCCGAGTATTAAAAAAATC (f), GCGCTCGAGTCATAATCCTTTTTTTTCTAATTTTTCCAGTATGGC (r), CATGTGCTGGCGGCGGTCCAGTATC (E388A/E389A, f), GATACTGGACCGCCGCCAGCACATG (E388A/E389A, r), GCTTCTGGAAGCAATGCTAACC (E414A, f), GGTTAGCATTGCTTCCAGAAGC (E414A, r), GGAACTGGCTTCAGTTGAAAC (D424A, f), GTTTCAACTGAAGCCAGTTCC (D424A, r), CGGCAGGCCGCAGCAGAGGCTG (R438A/K439A, f), CAGCCTCTGCTGCGGCCTGCCG (R438A/K439A, r), GTTTGTAAGATTGCGGCCATACTGG (Q446A, f), CCAGTATGGCCGCAATCTTACAAAC (Q446A, r), and CCTCGAGTCATAATCCTTTTTTTGCTAATTTTTCC (E453A, r). The products were purified by QiaQuick gel extraction kit (Qiagen), subcloned into the TOPO TA vector (Invitrogen) and sequenced. For *in vitro* binding assays, the fragments comprising wild type or mutant BAG4 BD were subcloned into the pGEX4T-1 vector and expressed in BL21(DE3) cells as GST-fusion proteins. After induction at room temperature with 0.1 mM isopropyl-1-thio-β-D-galactopyranoside, cells were lysed by sonication, and expressed proteins were isolated from lysates by affinity purification on glutathione-Sepharose (Amersham Biosciences). GST fusion proteins (5 μg) were immobilized on glutathione-Sepharose and incubated for 1 h at 4 °C in a volume of 0.1 ml of binding buffer (20 mM HEPES, pH 7.7, 142 mM KCl, 5 mM $MgCl_2$, 2 mM EGTA, 0.5% Nonidet P-40) with 1 μl of *in vitro* translated L-[^{35}S]methionine-labeled Hsc70 (pcDNA3-HA-Hsc70-(67–377), Ref. 11). The beads were then washed three times with 1 ml of ice-cold binding buffer, and bound proteins were separated by SDS-PAGE and visualized by autoradiography.

Computer Modeling—The homology models of BDs from BAG3 and BAG5 were created with SwissModel (22–24) using the sequence alignment shown in Fig. 2*c*. The coordinates were used to visualize charge and hydrophobicity distribution on molecular surfaces.

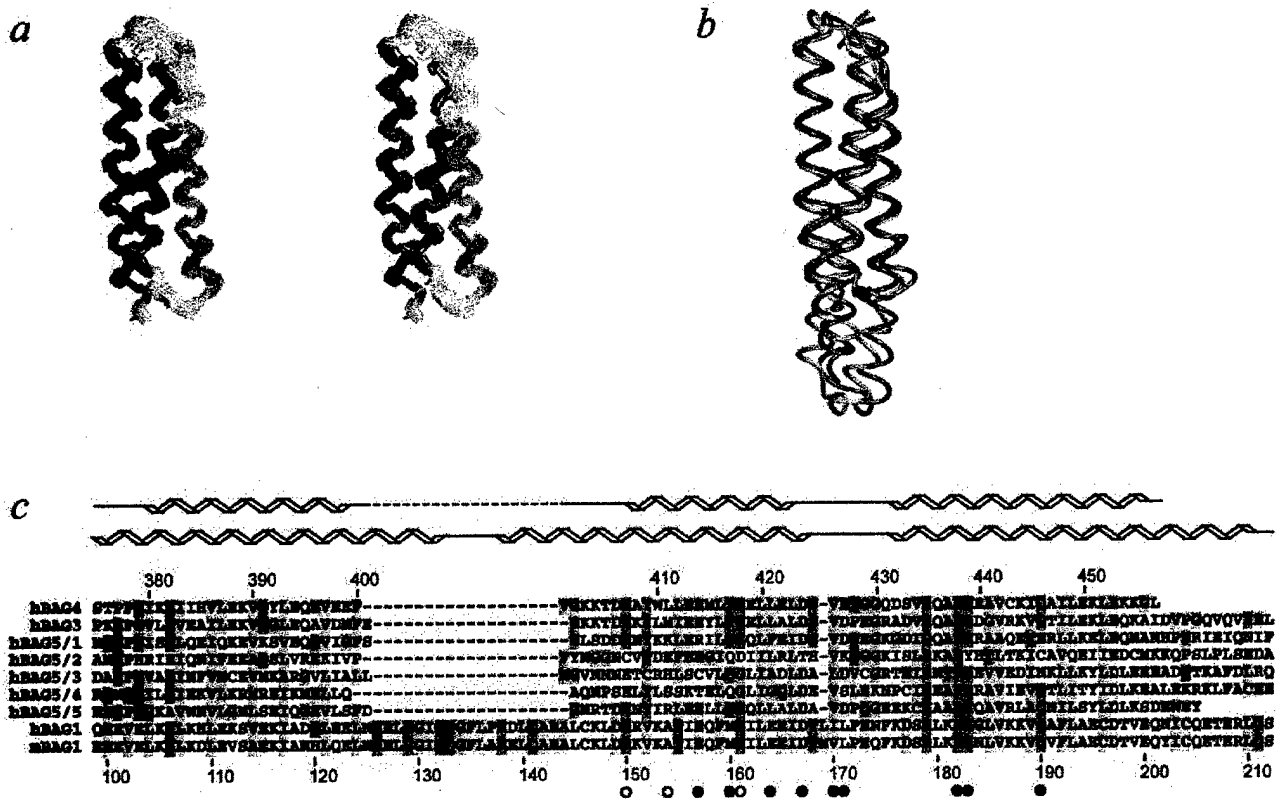

FIG. 2. **BAG domain from BAG4 is a short triple-helix bundle.** *a*, stereo view of 25 superimposed backbone traces of human BAG4 BD (residues 376–457). α1, *blue*; α2, *green*; α3, *red*; connecting loops, *yellow*; termini, *white*. *b*, comparison of BAG domains from BAG4 and BAG1. *Tube models* of Cα atoms from human BAG4 (*red*, residues 376–457), murine BAG1 (*blue*, PDB ID 1I6Z, residues 99–210), and human BAG1 (*green*, PDB ID 1HX1, residues 99–205) are shown[3]; the structures were superimposed using BAG4 backbone atoms located in α-helices (residues 380–399, 407–423, 432–456) and their counterparts in BAG1 proteins. Orientation of the molecules is the same as in *panel a*. *c*, structure-based sequence alignment of BAG domains. BDs from human BAG4 (hBAG4), human BAG3 (hBAG3), human BAG5 (hBAG5/1, hBAG5/2, hBAG5/3, hBAG5/4, and hBAG5/5), human BAG1 (hBAG1), and murine BAG1 (mBAG1) were aligned as described in the text. Homology is highlighted by the default ClustalX coloring scheme (27). Positions of residues in hBAG1 that interact with N- and C-terminal lobes of Hsc70 are indicated with *open* and *filled circles*, respectively. hBAG4 and mBAG1 residue numbers are marked *above* or *below* the respective sequences. Secondary structure of hBAG4 and mBAG1 BDs is outlined on *top*.

RESULTS AND DISCUSSION

Structure of the BAG Domain from BAG4—We have determined the solution structure of BAG4 BD, using multidimensional NMR methods. Similar to its BAG1 counterpart (3, 15), the BAG4 BD is a three-helix bundle (Fig. 2*a*). However, a striking difference between the BDs of BAG4 and BAG1 is obvious. The three helices in BAG4 BD, which correspond to residues 380–399 (α1), 407–423 (α2), and 432–456 (α3), are substantially shorter than those in BAG1 (Fig. 2*b*).

Comparison of BAG Domains from BAG1 and BAG4—To compare the BDs of BAG4 and BAG1, we first superimposed their structures using only residues that are identical in the most conserved helix α3. Once α3 was overlaid, structurally equivalent residues were matched in the whole domain. The resulting structure-based sequence alignment is shown in Fig. 2*c*. As the alignment illustrates, BAG4 BD, relative to BAG1, contains a deletion of 19 residues between α1 and α2. This deletion results in shortening of α1 and α2 by 2.5 and 3.5 turns, respectively. BAG4 BD also lacks three turns of the α-helix at the C-terminal end of α3. All three helices in BAG4 BD are truncated at one end of the structure, making the BD of BAG4 significantly shorter (26 × 12 × 11 Å) than the BD of BAG1 (37 × 14 × 10 Å).

After the two domains were superimposed, α1, α2, and α3 in BAG4 BD matched closely with their BAG1 counterparts (3, 15). The root mean square deviation (rmsd) of BAG4 backbone atoms in the three α-helices from equivalent atoms in murine and human BAG1 BD is 1.7 and 1.4 Å, respectively. (For comparison, rmsd between the same atoms of human and murine BAG1 is 1.2 Å). Also, the conformation of the loop between helices α2 and α3 is very similar in BAG4 and BAG1, even though it contains a single insertion, Met-169,[3] in the latter. Overall, the structure of BD from BAG4 closely resembles the upper two-thirds of the BAG1 BD (Fig. 2*b*).

Hsc70 Binding Interface on BAG4 BD—Most BAG1 residues that interact with Hsc70 (3) are conserved or are conservatively substituted in BAG4 BD (Fig. 2*c*). Hence, it can be predicted that BAG4 binds Hsc70 in a manner analogous to BAG1 (3, 15). This was tested experimentally by NMR-monitored titrations of BAG4 BD with a synthetic peptide corresponding to an α-helix (residues Asn-256–Cys-267) from the BAG1-binding interface on the ATPase domain of Hsc70. This helix contributes several predominantly basic residues to the intermolecular contacts with BAG1. In particular, Arg-258, Arg-261, Arg-262, and Thr-265 from Hsc70 form salt bridges with Glu-157, Glu-164, and Asp-167 from α2 and Asp-197 from α3 of BAG1

[3] The sequence numbering for murine BAG1 is the same as that used in our previous NMR study reporting the solution structure of mBAG1 (15). Human BAG1 is numbered accordingly for clarity. When the crystal structure of human BAG1 was published (3), a different numbering scheme was used based on the sequence of BAG1M, a longer isoform of BAG1. For direct comparison with the sequence numbers for human BAG1 in the crystal structure, the reader should add 55 to the BAG1 sequence numbers used in the present study.

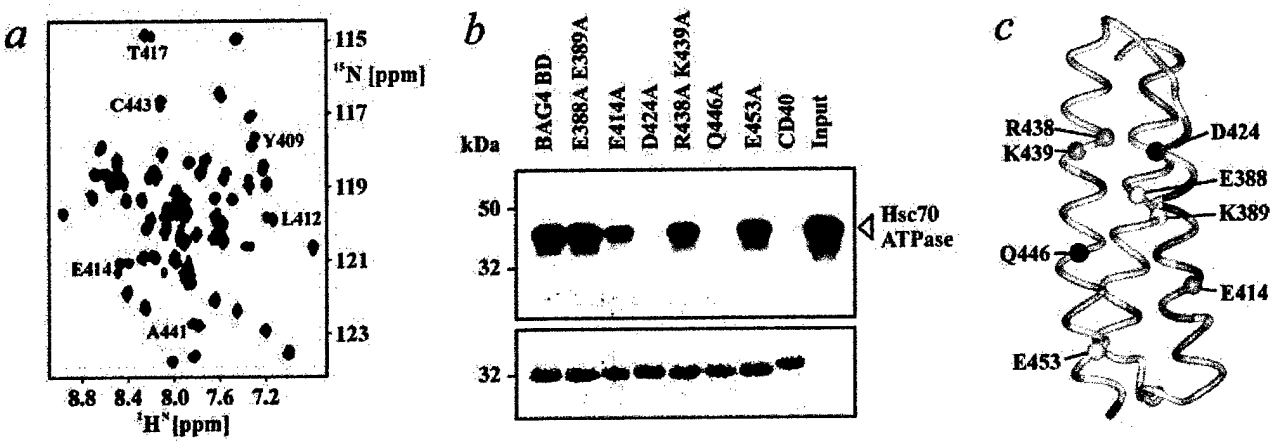

FIG. 3. **Analysis of BAG4 binding to Hsc70.** *a*, effect of Hsc70 peptide Asn-256–Cys-267 on ^{1}H-^{15}N HSQC spectra of BAG4 BD. Spectra of ligand-free BAG4 BD (*black*) and BAG4 BD in the presence of 30-fold molar excess of the peptide (*red*) are superimposed; several noticeable cross-peak shifts are labeled. *b*, mutational analysis of the interaction between human BAG4 BD and Hsc70. GST fusion proteins representing wild type BAG4 BD, mutants, or the CD40-negative control were immobilized on glutathione-Sepharose beads and tested for *in vitro* binding to *in vitro* translated L-[^{35}S]methionine-labeled Hsc70-(67–377). Samples were analyzed by SDS-PAGE and autoradiography to detect bound Hsc70 (*upper panel*) and with Coomassie Blue staining to verify loading of equivalent amounts of GST fusion proteins (*lower panel*). Substitutions for residues 388–389 were made as control mutations because they are located in α1, on the opposite side of the molecule from the Hsc70 contact interface, and were not expected to affect binding. *Input lane* shows one-fifth of the total *in vitro* translated protein, which was mixed with the GST fusion protein. *c*, *tube model* of BAG4 BD (residues 376–457) colored according to ^{1}H- and ^{15}N-chemical shift changes of the individual residues upon binding of the Hsc70 peptide Asn-256–Cys-267. Color intensity is proportional to the observed change. Sites of alanine substitution, which are described in *panel b*, are depicted as *spheres*. *Black*, *gray*, or *white spheres* indicate mutations that abolished, weakened, or did not affect binding to Hsc70, respectively. The chemical shifts and mutations that affect binding are located in α2-α3, marking an interaction interface that is closely similar to that seen in BAG1 (3, 15). Orientation of the molecule is the same as in Fig. 2.

(3). The peptide interacted with BAG4 BD; the most pronounced ^{1}H/^{15}N chemical shift changes in BAG4 BD induced by peptide binding were localized in α2 (Fig. 3, *a* and *c*). This is consistent with the expected peptide contact sites and with the results of NMR titrations of BAG1 with the same peptide (15).

To further define the binding interface in BAG4 BD across the conserved helices α2 and α3, we used site-directed mutagenesis of the predicted contact residues within these helices. The results indicated that Glu-414 and Asp-424 from α2, as well as Arg-438, Lys-439, and Gln-446 from α3 are important for the interaction of BAG4 with Hsc70, because mutating these residues to alanine abolished or weakened the binding (Fig. 3, *b* and *c*). The equivalents of these residues in BAG1 each make direct contact with Hsc70 (3). As expected, mutations in α1 (E388A, E389A) had no effect, because this helix does not interact with Hsc70. Thus the results indicate that the binding surface for the heat shock chaperone is similar in BAG4 and BAG1, involving α2-α3 and extending through an area of ~10 × 30 Å across one face of the domain.

Whereas most intermolecular interactions between BAG4 and Hsc70 are identical to those in the BAG1·Hsc70 complex (3), the contributions and relative importance of some residues differ. For example, the BAG4 E453A mutant still interacted with Hsc70, even though mutation of the equivalent residue in BAG1 (D197A, made as a double mutant with Q201A) resulted in a failure to bind Hsc70 (15). In BAG1, Asp-197 forms a salt bridge with Arg-258 in Hsc70 whereas Gln-201 is not involved in direct contact (3). Aspartic or glutamic acid is found at this position in all human BDs. It is possible that the longer aliphatic side chain of glutamic acid precludes formation of a stable intermolecular salt bridge as seen in the BAG1·Hsc70 complex, and consequently, this residue is not critical for BAG4·Hsc70 recognition.

Structure-based Sequence Alignment of Human BAG Domains—The sequence similarity between BDs of BAG4 and BAG1 is strongest in α3 (30% identical) and somewhat weaker in α2 (24% identical), so the alignment was clear for these two helices. However, until now, low levels of homology for the sequences in α1 obscured alignments of this region, even with knowledge of the BAG1 structure (1–3). In some cases, this segment of BDs was excluded from sequence alignments. Now, with the structures of two BDs in hand, it is possible to evaluate the conserved folding pattern of α1 and to more accurately predict sequence homology for the BDs. A structure-based sequence alignment is presented in Fig. 2*c*. The most significant correction to previous alignment attempts is the relative position of α1; BAG4 α1 spans residues 380–399, corresponding to structurally equivalent residues 104–123 in BAG1.

Whereas the sequence alignment of more distantly related BAG4 and BAG1 BDs required comparison of their structures, sequences of BDs from BAG3, BAG4, and BAG5 can be aligned with a high degree of confidence (Fig. 2*c*, compare with Refs. 2 and 3). BDs from BAG3 and BAG4 are the most closely related among human BDs, being 60% identical. BAG5 was shown previously to contain four BDs (20–40% identical to BAG3 and BAG4) (1, 2), arranged in tandem and accounting for most of the protein. Now, our alignment has revealed that another segment in BAG5, located immediately after the first BD and predicted to contain three α-helices, is yet another BD, which we termed BAG5/BD2. For the alignment in Fig. 2*c*, we renumbered the remaining BDs from the identifiers cited previously (2, 10) to BAG5/BD3, BAG5/BD4, and BAG5/BD5. The role of these linked BDs in BAG5 is not yet understood.

Alignment of the putative BDs from BAG2 and BAG6/Scythe was not straightforward, and therefore we did not include their sequences in Fig. 2*c*. Even though both proteins bind to Hsc70 and inhibit its refolding activity (1, 9), they are obvious outliers and their structures are likely to be different from other BDs. In BAG2, the C terminus of the protein itself terminates the putative BD shortly after the segment with homology to α2. Thus, if the folding pattern were retained for the first part of the domain, BD in BAG2 would lack most of α3. In contrast, the BD of BAG6 may lack the structural equivalent of α1 because the corresponding sequence contains several prolines that are likely to disrupt the helix. Only half of the residues whose counterparts in BAG1 contact the chaperone are conserved in

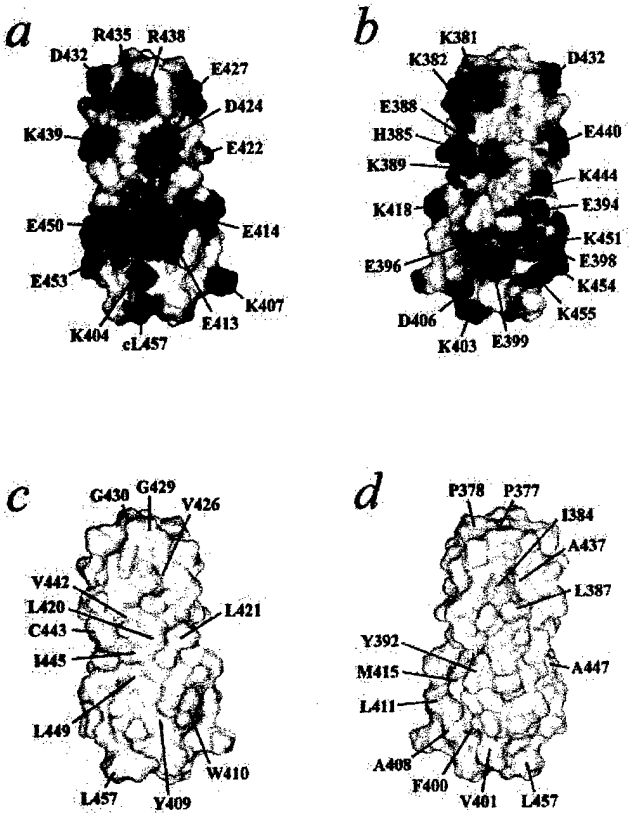

FIG. 4. **Surface maps of BAG4 BD.** In *panels a* and *b*, the solvent accessible surface of the domain is colored according to electrostatic potential. Areas with negative, positive, or neutral character are depicted in *red*, *blue*, or *white*, respectively. In *panel a*, the view is the same as in Fig. 2, with helices 2 and 3 and the Hsc70 binding site facing forward. In *panel b*, the molecule is rotated 180° around a vertical axis relative to the view in *panel a*, thus revealing the opposite side with helix 1 in front. In *panels c* and *d*, the surface is colored according to hydrophobicity. *Yellow color* intensity is proportional to increasing hydrophobic character, and the *front* and *back views* of the molecule are displayed as in *panels a* and *b*. Charged and hydrophobic residues are labeled in the appropriate panels.

BAG6. The region with α2-α3 homology is necessary for the binding of BAG6 to Hsc70 (9). It remains to be seen whether this segment forms a structural domain *per se* or is part of a novel larger domain, together with the preceding proline-rich region or other parts of the protein.

Implications for Human BAG Proteins—To consider conserved structure/function relationships in the human BAG family, we used BAG4 BD as a template to construct three-dimensional homology models for the BDs from BAG3 and BAG5. The sequence identity is 60, 39, 29, 22, 23, and 43% for BAG3 BD, BAG5/BD1, BAG5/BD2, BAG5/BD3, BAG5/BD4, and BAG5/BD5, respectively. The BDs from BAG2 and BAG6 were excluded from this comparison because they lack the clear homology seen in the other members of the family. Thus, a "gallery" of BDs was generated consisting of three experimentally determined structures (BAG4, murine BAG1, Ref. 15 and human BAG1, Ref. 3) and six homology models (Figs. 4 and 5). This gallery was used to compare the overall globular shape as well as surface features and protein interaction interfaces across the family. It should be noted for the homology models that the main chain conformation is likely to be accurate, but the positions of the side chains are less well defined. Our models provide a reasonable representation of overall surface feature distribution and can be useful in the absence of experimental structures of other members of the BAG family. BAG1, BAG3, and BAG4 interact with Hsc70 (1, 2, 6, 11, 20), and, consistent with that, the Hsc70-binding faces (helices α2 and α3) of BDs from these family members are very similar with respect to charge distribution (Fig. 5, *top row*). Acidic residues (Glu-413 and Glu-414 from α2, Asp-424 and Glu-427 from the connecting loop, and Glu-450 and Glu-453 from α3 in BAG4) dominate diagonally across the surface (Fig. 4*a*). The N-terminal portion of α3 presents a cluster of basic residues (Arg-435, Arg-438, and Lys-439 in BAG4), seen in the upper left corner of the domain (Fig. 4*a*). Some of the acidic residues and the basic cluster on the α2-α3 face are shared by all the BDs. Similarly, a central hydrophobic region (Leu-420 and Leu-421 from α2 and Val-442, Ile-445, and Leu-449 from α3 in BAG4) is conserved through the family (Fig. 5).

Among the BAG5 BDs, BAG5/BD5 is the most canonical whereas BAG5/BD2 is the least. In fact, the charge distribution in BAG5/BD2 is rather unusual, resulting in a large dipolar moment on the α2-α3 face of the domain. In BAG5/BD3 and BAG5/BD4, the cluster of acidic residues on α2 and α3 is not conserved, which could impede the interaction with Hsc70. In particular, the equivalents of the critical contact residue Glu-414 in BAG4 are cysteine in BAG5/BD3 and threonine in BAG5/BD4. When this glutamic acid is mutated to alanine in BAG4 or BAG1, binding to Hsc70 is abolished. The putative Hsc70 contact interfaces in BAG5/BD5 and also BAG5/BD1 are more closely similar to that in BAG4. In BAG5/BD5, this critical glutamate residue is conserved but an arginine is present at this site in BAG5/BD1. Interestingly, both of these BDs bind Hsc70 in *in vitro* assays.[2] Future studies are needed to reveal how BAG5 is organized, whether its five BDs act independently or interact with one another, and to identify the molecular targets of BAG5/BDs that do not bind Hsc70.

Short Versus Long BAG Domains—In our comparison of BDs from human BAG family members, we have demonstrated the presence of two structurally distinct BAG domains that divide the family into two subfamilies, characterized by the presence of "short" (BAG3, BAG4, and BAG5) or "long" (BAG1) BAG domains. Gene structure of these two BD types also differs and reflects separate evolutionary history. Whereas the BDs in BAG3, BAG4, and BAG5 are neither flanked by nor contain any introns, there are several phase 0 introns in the BD region of the human *BAG1* gene. The existence of short and long varieties raises numerous questions about evolution and function of BDs. Because the short BD is sufficient for binding to Hsc70 and modulating its activity, what is the advantage of having each α-helix extended at one end of the long BD by three turns? Does the long BD represent the original form, and did the short BD arise by elimination of the part of the molecule that was not required for its function? Alternatively, did the long BD evolve from an ancestral short BD, with the extra residues enabling it to gain a new function?

To learn more about short and long BDs, we investigated which types are present in other species. Sequences similar to BDs are found in fungi, plants, and animals (1–3). Proteins containing the long BD, homologous to human BAG1, have been identified in various vertebrates (mouse, *Mus musculus*, Ref. 4; rat, *Rattus norvegicus*, BI280304, BF407193, AI045819; cow, *Bos taurus*, AV601527; frog, *Xenopus* laevis, AW640566, BJ036536; fish, *Oryzias latipes*, BJ021354) and in nematodes (*Caenorhabditis elegans*, Ref. 1; *Meloidogyne arenaria*, BI746004, BI501569; *Meloidogyne javanica*, BI324599; *Heterodera glycines*, BF249474). All the nematode BDs contain an insertion of 6 residues between α2 and α3. Short BDs, similar to those in human BAG4, have been found throughout vertebrates (mouse, *M. musculus*, BAB27167; rat, *R. norvegicus*, BF392489; cow, *B. taurus*, BM104841, AW416999; chicken,

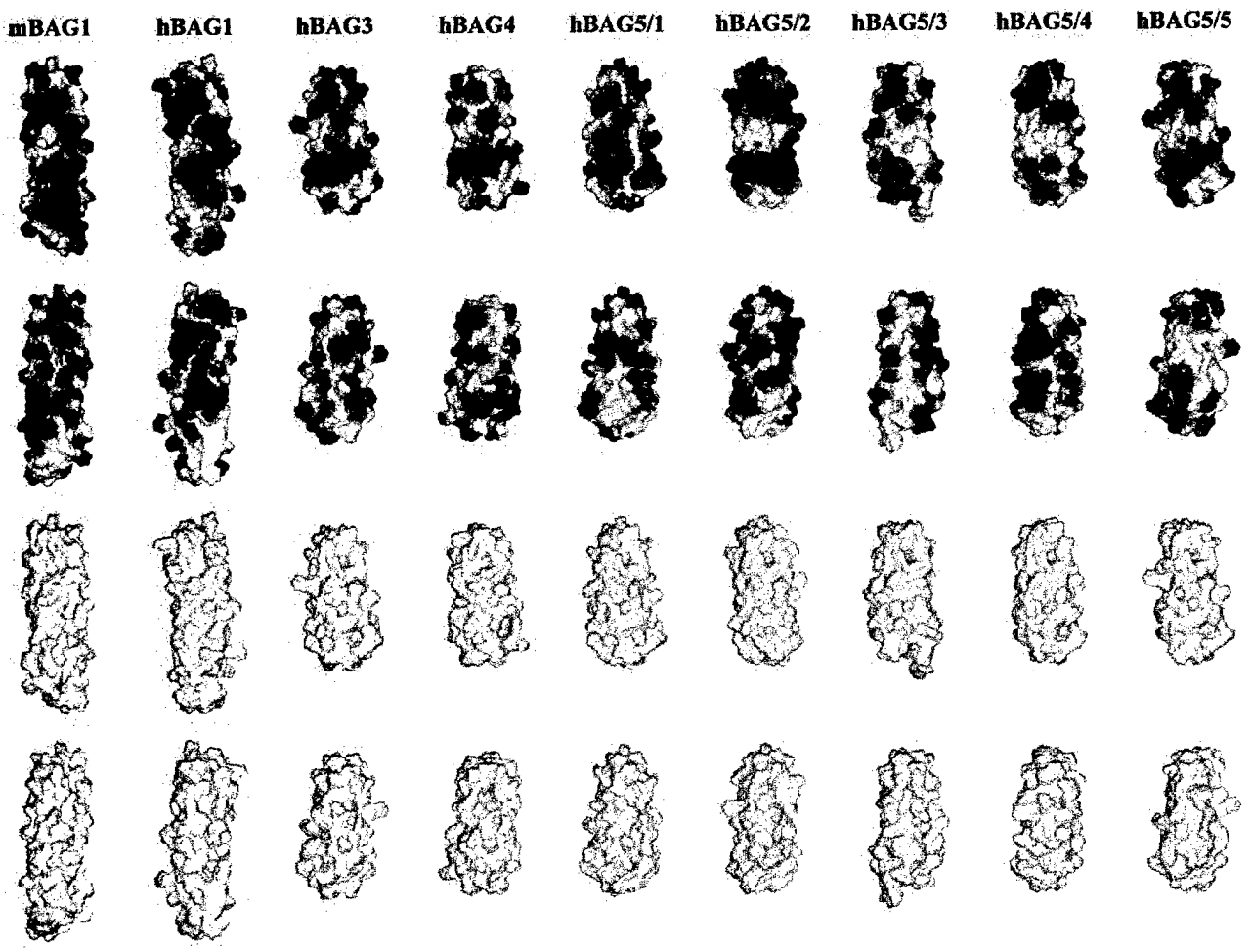

FIG. 5. **A comparative gallery of BAG domains.** Contact surfaces of BDs from BAG1, BAG3, BAG4, and BAG5 (*columns 1–9*), whose sequences are aligned in Fig. 2, are colored according to electrostatic potential (*rows 1* and *2*) and hydrophobicity (*rows 3* and *4*). Residues 99–210 of murine BAG1 (PDB ID 1I6Z), residues 99–205 of human BAG[3] (PDB ID 1HX1), residues 376–457 of human BAG4, and corresponding residues from homology models of BAG3 and BAG5 BDs are shown. Coloring and orientation are the same as in Fig. 4 to permit direct comparison. *Front views* are shown in *rows 1* and *3*, whereas *back views* are presented in *rows 2* and *4*.

Gallus gallus, AJ396368; zebrafish, *Danio rerio*, BM071126, BG303781, BM095203) and in chordates (tunicate, *Ciona intestinalis*, AV841356, AV881072). Short BDs are also present in insects (silkworm, *Bombyx mori*, Ref. 21; fruit fly, *Drosophila melanogaster*, Ref. 3; bee, *Apis mellifera*, BI515842, BI508980; mosquito, *Anopheles gambiae*, AJ280648) in a set of proteins distinct from BAG3, BAG4, and BAG5. In BDs from fungi (Snl1p in *Saccharomyces cerevisiae* (2); BAG1A and BAG1B in *Schizosaccharomyces pombe* (1); *Neurospora crassa*, CAB88563), homology is limited to the Hsc70-binding region of α2 and α3, which is common to both short and long BDs. However, the C termini of the proteins limit α3 to a size typical of a short BD. Consistent with this observation, secondary structure prediction indicates that the three α-helices span a region of approximately 90 residues. Altogether, BDs in fungi are likely to be short. Also in plant BDs (2, 3), only the chaperone-binding sequence of α2 and α3 is conserved. In this case, however, protein termini do not limit the size of the BDs, and secondary structure prediction is not straightforward. Classification as short or long may therefore require knowledge of the three-dimensional structure of these proteins.

The presence of the short BD in at least two kingdoms, animals and fungi, suggests that this form of BD is of ancient origin. It is not clear if the long BD is limited only to a part of the animal kingdom, or if it will be found elsewhere as well. Interestingly, nematodes possess an orthologue of BAG1, which contains the long BD, but the short BD has not yet been identified in the completed genome of *C. elegans*. Does this imply that the short BD is absent in some animal species? Obviously, many open questions remain. The origin of short and long BDs, point of their divergence, diversity of BDs within eukaryotes, and significance of their different lengths are still obscure. Also, even though the structures of BAG domains from human and mouse BAG1 (3, 15) and from human BAG4 have been determined, it is not straightforward to predict structures of BDs from distantly related BAG family members whose sequence similarity is limited to Hsc70-binding regions of α2 and α3. Once the structures of BDs from yeast and plant proteins, as well as those from BAG2 and BAG6, are known they will provide new insights into the structure-function relationship in this diverse family of molecular regulators.

Acknowledgments—We thank N. E. Preece for assistance with the Varian 500 MHz spectrometer, D. Kedra for help with sequence database searches, J. C. Reed for helpful discussions and critical review of the manuscript, and S. Hammond for assistance in preparing the manuscript for publication. This research was performed in part at the Environmental Molecular Sciences Laboratory (a national scientific user facility sponsored by the United States DOE Office of Biological and Environmental Research) located at Pacific Northwest National Laboratory, operated by Battelle for the DOE.

REFERENCES

1. Takayama, S., Xie, Z., and Reed, J. (1999) *J. Biol. Chem.* **274,** 781–786
2. Tschopp, J., Martinon, F., and Hofmann, K. (1999) *Curr. Biol.* **9,** R381–384
3. Sondermann, H., Scheufler, C., Schneider, C., Höhfeld, J., Hartl, F.-U., and Moarefi, I. (2001) *Science* **291,** 1553–1557
4. Takayama, S., Sato, T., Krajewski, S., Kochel, K., Irie, S., Millan, J. A., and Reed, J. C. (1995) *Cell* **80,** 279–284
5. Lee, J. H., Takahashi, T., Yasuhara, N., Inazawa, J., Kamada, S., and Tsujimoto, Y. (1999) *Oncogene* **18,** 6183–6190
6. Doong, H., Price, J., Kim, Y. S., Gasbarre, C., Probst, J., Liotta, L. A., Blanchette, J., Rizzo, K., and Kohn, E. (2000) *Oncogene* **19,** 4385–4395
7. Jiang, Y., Woronicz, J. D., Liu, W., and Goeddel, D. V. (1999) *Science* **283,** 543–546
8. Thress, K., Henzel, W., Shillinglaw, W., and Kornbluth, S. (1998) *EMBO J.* **17,** 6135–6143
9. Thress, K., Song, J., Morimoto, R. I., and Kornbluth, S. (2001) *EMBO J.* **20,** 1033–1041
10. Takayama, S., and Reed, J. C. (2001) *Nat. Cell Biol.* **3,** E237-E241
11. Takayama, S., Bimston, D. N., Matsuzawa, S., Freeman, B. C., Aime-Sempe, C., Xie, Z., Morimoto, R. J., and Reed, J. C. (1997) *EMBO J.* **16,** 4887–4896
12. Stuart, J. K., Myszka, D. G., Joss, L., Mitchell, R. S., McDonald, S. M., Zhihua, X., Takayama, S., Reed, J. C., and Ely, K. R. (1998) *J. Biol. Chem.* **273,** 22506–22514
13. Wang, H. G., Takayama, S., Rapp, U. R., and Reed, J. C. (1996) *Proc. Natl. Acad. Sci. U. S. A.* **93,** 7063–7068
14. Song, J., Takeda, M., and Morimoto, R. I. (2001) *Nat. Cell Biol.* **3,** 276–282
15. Briknarová, K., Takayama, S., Brive, L., Havert, M. L., Knee, D. A., Velasco, J., Homma, S., Cabezas, E., Stuart, J., Hoyt, D. W., Satterthwait, A. C., Llinás, M., Reed, J. C., and Ely, K. R. (2001) *Nat. Struct. Biol.* **8,** 349–352
16. Cornilescu, G., Delaglio, F., and Bax, A. (1999) *J. Biomol. NMR* **13,** 289–302
17. Brünger, A. T., Adams, P. D., Clore, G. M., DeLano, W. L., Gros, P., Grosse-Kunstleve, R. W., Jiang, J. S., Kuszewski, J., Nilges, M., Pannu, N. S., Read, R. J., Rice, L. M., Simonson, T., and Warren, G. L. (1998) *Acta Crystallogr. Sect. D,* **54,** 905–921
18. Koradi, R., Billeter, M., and Wuthrich, K. (1996) *J. Mol. Graph.* **14,** 51–55
19. Cabezas, E., and Satterthwait, A. C. (1999) *J. Am. Chem. Soc.* **121,** 3862–3875
20. Antoku, K., Maser, R. S., Scully, W. J. Jr., Delach, S. M., and Johnson, D. E. (2001) *Biochem. Biophys. Res. Commun.* **286,** 1003–1010
21. Moribe, Y., Niimi, T., Yamashita, O., and Yaginuma, T. (2001) *Eur. J. Biochem.* **268,** 3432–3442
22. Guex, N., Diemand, A., and Peitsch, M. C. (1999) *Trends Biochem. Sci.* **24,** 364–367
23. Guex, N., and Peitsch, M. C. (1997) *Electrophoresis* **18,** 2714–2723
24. Peitsch, M. C. (1995) *Bio/Technology* **13,** 658–660
25. Takayama, S., Krajewski, S., Krajewska, M., Kitada, S., Zapata, J. M., Kochel, K., Knee, D., Scudiero, D., Tudor, G., Miller, G. J., Miyashita, T., Yamada, M., and Reed, J. C. (1998) *Cancer Res.* **58,** 3116–3131
26. Yang, X., Chernenko, G., Hao, Y., Ding, Z., Pater, M. M., Pater, A., and Tang, S. C. (1998) *Oncogene* **17,** 981–989
27. Thompson, J. D., Gibson, T. J., Plewniak, F., Jeanmougin, F., and Higgins, D. G. (1997) *Nucleic Acids Res.* **24,** 4876–4882
28. Laskowski, R. A., MacArthur, M. W., Moss, D. S., and Thornton, J. M. (1993) *J. Appl. Cryst.* **26,** 283–291